Scilight

Energy, Water and Air Catalysis Research
https://www.sciltp.com/journals/ewacr

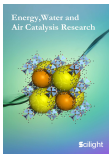

Review

Review of g-C_3N_4-Based Photocatalytic Systems: Design Strategies toward Sustainable Hydrogen Production

Yuvaraj M. Hunge [1,*,†], Anuja A. Yadav [2,†], Sutripto Majumder [3], Abdel Hamid I. Mourad [4], Akira Fujishima [1,5] and Chiaki Terashima [1,6]

[1] Research Center for Space System Innovation, Research Institute for Science and Technology, Tokyo University of Science, 2641 Yamazaki, Noda, Chiba 278-8510, Japan
[2] Faculty of Pure and Applied Sciences, University of Tsukuba, Tsukuba, Ibaraki 305-8573, Japan
[3] Department of Materials Science and Engineering, Chungnam National University, Daejeon 34134, Republic of Korea
[4] Department of Mechanical and Aerospace Engineering, College of Engineering, United Arab Emirates University, Al-Ain P.O. Box 15551, United Arab Emirate
[5] Institute of Photochemistry and Photomaterials, University of Shanghai for Science and Technology, Shanghai 200093, China
[6] Graduate School of Science and Technology, Tokyo University of Science, 2641 Yamazaki, Noda, Chiba 278-8510, Japan
* Correspondence: yuvarajhunge@gmail.com
† These authors contributed equally to this work.

How To Cite: Hunge, Y.M.; Yadav, A.A.; Majumder, S.; et al. Review of g-C3N4-Based Photocatalytic Systems: Design Strategies toward Sustainable Hydrogen Production. *Energy, Water and Air Catalysis Research* **2025**, *1*(1), 2.

Received: 26 August 2025
Revised: 12 November 2025
Accepted: 13 November 2025
Published: 19 November 2025

Abstract: With growing concerns over the global energy crisis and environmental degradation, there is an urgent push toward cleaner and more sustainable energy sources. Among the promising solutions, photocatalytic water splitting has emerged as an eco-friendly method for hydrogen production by harnessing sunlight. However, traditional photocatalysts like TiO_2, ZnO, and CdS face notable limitations, such as poor visible light absorption, fast electron-hole recombination, and stability issues under long-term use. Graphitic carbon nitride (g-C_3N_4), a metal-free semiconductor with a two-dimensional structure, has gained attention due to its favorable band gap, good thermal and chemical stability, and ease of synthesis. Still, its photocatalytic performance in its pure form remains limited, mainly due to low charge separation efficiency and insufficient surface activity. To overcome these drawbacks, researchers have explored a variety of modification strategies such as tuning the morphology, doping with elements, coupling with co-catalysts, and building heterojunctions. These approaches have shown great potential in improving light absorption, charge carrier mobility, and the overall hydrogen evolution efficiency. This review highlights recent progress in developing and modifying g-C_3N_4 based materials for photocatalytic hydrogen production. It explores how different structural and electronic modifications impact performance and delves into the mechanisms behind these improvements. Challenges such as long-term stability, cost-effectiveness, and scalability are discussed, along with potential strategies to address them. Looking ahead, more focus is needed on large-scale synthesis, durability in real-world conditions, and integrating these materials into practical systems to truly unlock the potential of g-C_3N_4 in sustainable hydrogen production.

Keywords: graphitic carbon nitride; photocatalytic hydrogen production; element doping; cocatalyst heterojunction

1. Introduction

The escalating global energy crisis and environmental degradation underscore the urgent need for cleaner, sustainable energy. The International Energy Agency projects a 25% rise in global energy demand by 2040, with fossil fuels remaining the dominant source. This continued reliance not only accelerates carbon emissions but also heightens the risk of climate change. Hydrogen has emerged as a key player in the shift toward low-carbon energy systems. Its clean-burning nature and versatility make it valuable across a wide range of sectors, from heavy industry and transportation to power generation and construction [1–4]. To ensure energy security and reduce dependence on any single source, hydrogen production must be diversified drawing from renewables, natural gas, and even coal-based methods. As countries work toward carbon neutrality, hydrogen is expected to play a central role in the future energy mix. However, most current hydrogen production processes, especially those based on fossil fuels, come with serious drawbacks. They emit significant amounts of CO_2, suffer from low energy efficiency, and produce harmful pollutants like sulfur and nitrogen compounds. These processes are also costly and heavily reliant on non-renewable resources. While they've met demand so far, their environmental impact is a growing concern. Biological methods offer a greener alternative, but issues like low yield and complex operation have limited their practical use [5–10]. This makes it all the more urgent to develop advanced technologies that can deliver hydrogen efficiently without harming the environment. Photocatalysis is one such promising solution. It runs on sunlight, uses abundant materials, and requires relatively low energy input, making it a strong candidate for sustainable hydrogen production. Photocatalytic water splitting, which uses sunlight to drive the decomposition of water into hydrogen and oxygen, presents a clean and sustainable alternative to conventional hydrogen production. Unlike fossil fuel-based methods, it avoids high carbon emissions, low energy efficiency, and the release of harmful pollutants. Additionally, it offers several advantages over biological hydrogen production, including higher yields, simpler operation, and better technological scalability [11–13]. These benefits have positioned photocatalysis as a promising and widely researched strategy for green hydrogen generation.

Photocatalytic water splitting combines electrochemical and photophysical processes to generate hydrogen using organic semiconductor photocatalysts. As a thermodynamically uphill reaction, it requires a minimum energy input of 1.23 eV (ΔG = 1.23 eV), corresponding to the standard redox potentials of water: 0 V for H_2O/H_2 and 1.23 V for H_2O/O_2. To drive this reaction, the photocatalyst must have a band gap exceeding 1.23 eV and the ability to absorb light below 1000 nm. Accounting for overpotentials, a practical band gap is typically >1.8 eV. For visible-light activity ($\lambda > 400$ nm), the band gap should be <3.0 eV [14–16], with an ideal range of 1.8–2.2 eV for efficient solar energy conversion. Photocatalytic hydrogen production efficiency depends not only on band structure but also on kinetics like charge transfer, separation, and surface redox reactions. The process involves four main steps: photon absorption, charge separation, charge transport, and catalytic reaction at active sites [17] (Figure 1). Upon illumination, photons excite electrons from the valence band to the conduction band (with a band gap of 1.8–2.2 eV), creating electron–hole pairs that migrate to the catalyst surface to drive gas production.

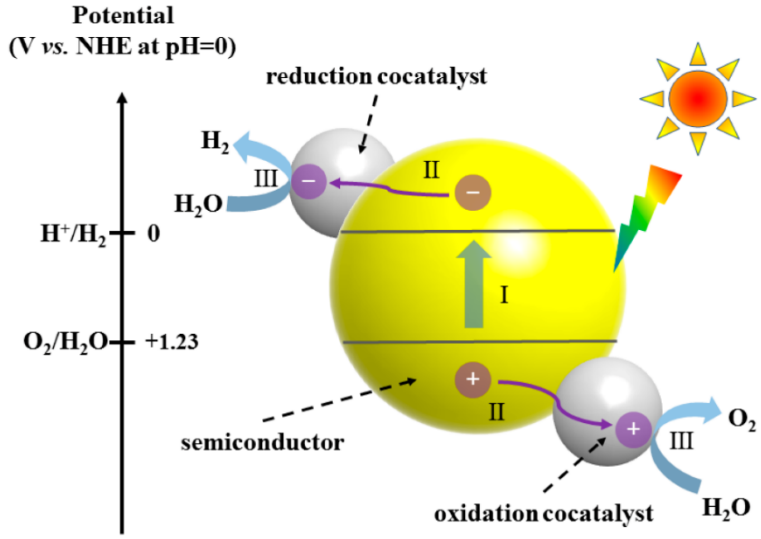

Figure 1. Overview of photocatalytic H_2 production of semiconductor. Reproduced with permission from [12]. © 2024 by the authors, licensed under CC BY 4.0.

During this process, electron–hole pairs may recombine quickly due to a small band gap and short lifetime, limiting effective carriers reaching the surface and reducing gas production. Water molecules adsorbed on the photocatalyst surface undergo redox reactions: holes oxidize water into O_2 and H^+, while electrons reduce H^+ to H_2. This step depends on the photocatalyst's active sites, reaction conditions, and reactant adsorption [18]. Thus, improving water photolysis efficiency requires careful consideration of these factors.

For years, scientists have focused on designing semiconductor materials capable of splitting water under ultraviolet or visible light illumination. However, many traditional metal-based semiconductors such as TiO_2 (~3.2 eV), ZnO (~3.4 eV), WO_3 (~3.2 eV), and $BiVO_4$ (~2.9 eV) suffer from wide band gaps that limit their ability to harvest visible light efficiently. This has restricted their practical application, especially on an industrial scale. To overcome this challenge, attention has shifted to semiconductors with narrower band gaps, including metal sulfides, phosphides, and nitrides like CdS (~2.4 eV), SnS_2 (~1.7 eV), Ni_2P (~1.0 eV), InP (~1.4 eV), and InN (~1.1 eV) [19]. These materials offer better solar absorption and appropriate band positions for hydrogen evolution. However, issues like photo-corrosion and instability under operating conditions continue to hinder their widespread use. A significant milestone was reached in 2009 when Wang et al. [20] demonstrated that graphitic carbon nitride (g-C_3N_4) could drive hydrogen production under visible light. Since then, g-C_3N_4 has gained attention as a next-generation photocatalyst due to its many appealing properties: simple synthesis routes, abundant and inexpensive precursors, excellent chemical and thermal stability, and a band structure well-aligned for photocatalytic water splitting. These qualities make g-C_3N_4 a leading candidate for scalable and sustainable hydrogen production in the coming years ahead. g-C_3N_4 has recently gained attention as an efficient photocatalyst for solar-driven hydrogen production. With a moderate band gap of ~2.7 eV, it absorbs a broader range of visible light than TiO_2 (~3.2 eV), enhancing solar energy utilization. Unlike metal sulfides such as CdS (~2.42 eV), g-C_3N_4 is metal-free, environmentally benign, and highly stable in water, showing strong resistance to photo-corrosion during prolonged operation. [21,22]. g-C_3N_4 remains a cost-effective and environmentally benign alternative with significant room for improvement. One widely used strategy to enhance its performance involves constructing heterojunctions by coupling g-C_3N_4 with other semiconductors like TiO_2, ZnO, or noble metals like Pt, Au [21–25]. These combinations improve charge separation and mobility, which are crucial for boosting photocatalytic efficiency. Additionally, g-C_3N_4-based composites can broaden light absorption and introduce new active sites, further improving their catalytic performance. These modifications effectively address the inherent drawbacks of pristine g-C_3N_4 and offer practical routes toward high-efficiency, stable hydrogen production systems. Beyond hydrogen evolution, g-C_3N_4-based materials are also explored for applications in organic pollutant degradation, although their use in gas sensing and supercapacitors remains relatively unexplored.

This review presents a comprehensive and up-to-date overview of g-C_3N_4-based composite photocatalysts for hydrogen generation, emphasizing the interplay between material design and photocatalytic mechanisms. It systematically discusses both conventional strategies such as cocatalyst modification, elemental doping, and heterojunction engineering and emerging approaches including single-atom catalysis, plasmonic enhancement, and defect modulation. Distinct from previous reviews, this work focuses on the structure activity relationship and highlights sustainability, scalability, and practical feasibility, providing a unified perspective for the rational design of next-generation, high-performance g-C_3N_4-based photocatalytic systems.

2. Structure of g-C_3N_4

Graphitic carbon nitride (g-C_3N_4) is widely recognized for its excellent photocatalytic capabilities, making it a valuable material for environmental purification and energy conversion technologies [26]. It stands out due to its broad light absorption in the visible range, chemical robustness, and low production cost. The material's covalently bonded carbon and nitrogen framework helps facilitates the separation of photo-generated electron hole pairs, which is essential for improved photocatalytic performance [27]. However, g-C_3N_4 still faces challenges, particularly its relatively low electron mobility and tendency of charge carriers to recombine, both of which limit its efficiency.

Structurally, g-C_3N_4 is composed of layered carbon–nitrogen sheets arranged in a graphite-like planar structure (Figure 2) [28]. The layers are bound by weak van der Waals forces, making the material easily exfoliable and highly tunable for catalytic applications. This layered arrangement provides abundant active sites for photocatalytic reactions, contributing to improved surface activity [29].

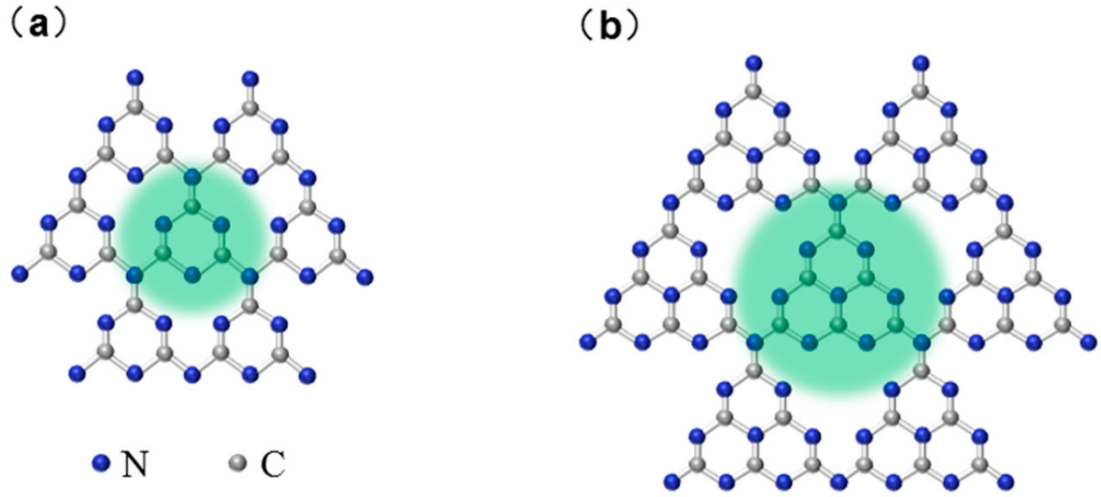

Figure 2. Molecular structure of *g*-C_3N_4: (**a**) triazine structure (C_3N_3); (**b**) tri-s-triazine structure (C_6N_7). Reproduced with permission from [12]. © 2024 by the authors, licensed under CC BY 4.0.

Nevertheless, the inherently low specific surface area of bulk g-C_3N_4 restricts the number of accessible active sites and reduces interactions between the catalyst and reactants. To address this, researchers have focused on engineering the material into porous, nanoscale, or ultrathin forms, which significantly enhances surface area and overall photocatalytic efficiency. Although several synthesis routes have been explored, many conventional methods such as hydrothermal synthesis and chemical vapor deposition (CVD) have drawbacks related to energy demand, scalability, and environmental impact. Hydrothermal methods often require high temperatures and pressures, limiting industrial viability. CVD offers precise control over material properties but requires high energy input and has low precursor utilization efficiency. Additionally, many of these techniques rely on toxic solvents or generate harmful byproducts, raising safety and sustainability concerns. To overcome these limitations, recent developments in green synthesis approaches such as mild solvothermal processes, microwave-assisted synthesis, and bio-templating have shown great promise. These methods not only lower energy consumption and reduce waste but also improve scalability and environmental compatibility. As such, they offer a promising pathway toward the large-scale, sustainable production of high-performance g-C_3N_4 for clean energy and environmental applications.

2.1. Preparation Methods of g-C_3N_4

g-C_3N_4 is a versatile material known for its outstanding photoelectric properties, and it is widely used in applications ranging from photocatalysis and water splitting to gas sensing. Various synthesis techniques have been developed to produce g-C_3N_4, each offering specific advantages and presenting certain limitations. Common preparation methods include high-temperature solid-state reactions, solvothermal and hydrothermal synthesis, template-assisted methods, and chemical vapor deposition (CVD) [30]. Each of these approaches differs in terms of reaction conditions, energy efficiency, product yield, and environmental impact. Five primary synthesis methods are used for preparing g-C_3N_4, each with specific advantages and drawbacks. The solid-state reaction involves calcination at 500–600 °C in an inert atmosphere (N_2 or Ar). It is simple and reliable but consumes high energy and may generate impurities [31]. The solvothermal method, conducted in solvents like water or alcohol at 200–300 °C, allows mild, controllable reactions but yields small quantities and may leave solvent residues [32]. The template method enables precise control of morphology and particle size using hard or soft templates, though the process is complex, costly ($10–20/g), and requires challenging template removal [33]. The hydrothermal approach, performed in aqueous media at 180–250 °C, provides tunable reaction conditions and high-quality materials but has low production efficiency (0.1–1 g/day) [34]. Lastly, chemical vapor deposition (CVD) produces uniform thin films or nanostructures under high temperatures and controlled atmospheres; however, it is expensive ($50–100/g) and technically demanding [35].

This comparison serves as a useful reference for selecting the most appropriate synthesis method depending on the desired application, material performance, and production scale. Although several synthesis methods have been effectively used to prepare g-C_3N_4 and similar materials, many still face significant challenges in scaling up to industrial production. High energy demands, low output yields, and environmental concerns continue to limit their large-scale implementation. For example, traditional hydrothermal synthesis requires high temperatures and pressures, making the process energy-intensive and difficult to scale due to the use of sealed reactors. Moreover,

many of these conventional approaches involve hazardous chemicals, toxic solvents, or produce environmentally harmful byproducts raising concerns related to both safety and sustainability. In response to these issues, recent research has focused on greener synthesis alternatives. Techniques such as mild-condition solvothermal processes, microwave-assisted rapid synthesis, and bio-templating have shown considerable promise. These methods reduce energy usage, improve material yield, and minimize environmental impact. The development of such eco-friendly and energy-efficient synthesis strategies provides a viable path forward for the sustainable and scalable production of high-performance materials. As these green technologies continue to advance, they are expected to play a key role in expanding the practical applications of g-C_3N_4 across fields such as clean energy, environmental remediation, and advanced functional materials.

3. Strategies for Enhancing Photocatalytic H_2 Production Performance of g-C_3N_4 Based Photocatalysts

g-C_3N_4 has gained attention for its excellent photoelectric properties and potential in photocatalytic hydrogen production. However, its practical use is limited by narrow light absorption, poor electron–hole separation, and low conductivity. To address these issues, strategies such as morphology control, doping, and heterojunction construction have been employed. Such strategies improve surface area, light absorption, charge transport, and stability, significantly improving photocatalytic efficiency and expanding its role in sustainable energy applications.

3.1. Morphology Control

Morphological engineering of graphitic carbon nitride (g-C_3N_4) is a powerful strategy to enhance its photocatalytic performance. As illustrated in Figure 3, tailoring the dimensional structure of g-C_3N_4 significantly influences its optical, electronic, and surface properties. Increasing the specific surface area not only exposes more active sites but also facilitates better light harvesting and improved charge carrier dynamics [36].

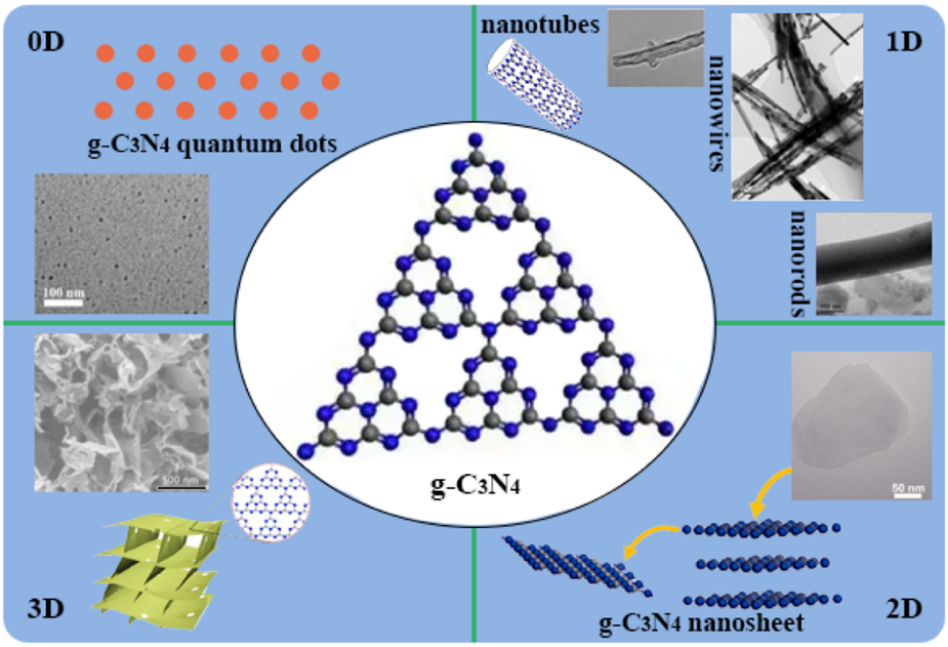

Figure 3. Schematic representation of zero, one, two and three dimensional (0D, 1D, 2D and 3D) g-C_3N_4. Reproduced with permission from [36]. © 2022 by the authors, licensed under CC BY 4.0.

Additionally, morphology modulation can extend visible-light absorption and reduce charge diffusion distances, promoting more efficient separation and transport of charge carriers. Zero-dimensional (0D) g-C_3N_4, typically synthesized in the form of quantum dots, exhibits strong quantum confinement, which contribute to enhanced catalytic activity and suitability for multifunctional applications such as photocatalysis and bioimaging [37]. One-dimensional (1D) architectures, including nanotubes, offer directed pathways for charge transport while suppressing electron–hole recombination. Key structural parameters—such as tube diameter (20–50 nm), wall thickness (5–15 nm), aspect ratio (>50), and surface area (>60 m^2/g) are known to influence catalytic efficiency. Narrow diameters and optimal wall thicknesses shorten charge migration paths and maintain mechanical integrity, while high aspect ratios and surface areas enhance carrier mobility and reactant adsorption [38]. Two-dimensional (2D) g-C_3N_4 nanosheets, due to their ultrathin profiles, exhibit improved charge separation and abundant surface-

active sites, making them ideal for light-driven reactions and sensor applications [39]. Three-dimensional (3D) configurations, formed via porous or hierarchical assembly, offer superior mass transport properties and mechanical stability, making them well-suited for scalable processes such as environmental remediation, adsorption, and energy storage [40].

Overall, the dimensional tuning of g-C_3N_4 from 0D to 3D enables precise control over its physicochemical behavior, allowing for the design of advanced materials tailored to specific energy conversion and catalytic applications. Such structural versatility presents a promising platform for future innovations in sustainable energy and environmental technologies.

3.2. Elemental Doping

Although morphology engineering such as creating nanosheets, nanotubes, or porous forms enhances the photocatalytic efficiency of g-C_3N_4 by increasing surface area and light absorption, it has limited impact on improving charge carrier separation. To address this limitation, elemental doping has become a widely adopted strategy to further optimize the electronic properties and boost overall photocatalytic performance. Elemental doping in g-C_3N_4 is generally categorized into metal doping, non-metal doping, and co-doping (metal/non-metal combination) [41]. Metal doping involves incorporating metal ions into the g-C_3N_4 matrix through various pathways:

(i) coordination with nitrogen atoms in the intrinsic cavities;
(ii) intercalation between the interlayer spaces; and
(iii) substitution of carbon or nitrogen atoms in the framework.

These interactions often result in the formation of metal nitrogen bonds, leading to modifications in the electronic band structure and improved charge carrier dynamics [42].

In non-metal doping, dopants can either intercalate between layers or substitute for C or N atoms in the lattice, forming new chemical bonds that influence the material's optical and electronic characteristics [43]. Co-doping, or dual-element doping, integrates both metal and non-metal elements into the g-C_3N_4 structure simultaneously. This approach leverages the synergistic effects of both dopants to fine-tune the band structure, improve charge carrier separation and mobility, and significantly elevate photocatalytic activity. These doping strategies offer a powerful means to overcome the intrinsic limitations of pristine g-C_3N_4, paving the way for the development of more efficient and stable photocatalytic systems.

3.3. Non-Metal Doping

Incorporating non-metallic elements into the g-C_3N_4 lattice can significantly modify its electronic structure, enabling fine-tuning of band edge positions, extending visible light absorption, and improving the separation and mobility of photogenerated charge carriers. Dopants such as boron (B), carbon (C), oxygen (O), sulfur (S) [44–48], and phosphorus (P) have been widely explored for their potential to enhance photocatalytic performance. Among them, carbon doping has shown particular promise. Hussain et al. [49] synthesized carbon-doped g-C_3N_4 (Cn-MA) by co-polymerizing melamine with sucrose, enabling in-situ self-doping. While single-element non-metal doping can enhance specific photocatalytic properties, its impact is often limited. To achieve broader and more synergistic improvements, dual or multi-element non-metal co-doping has emerged as a more effective approach. This technique allows for simultaneous tuning of multiple physicochemical parameters, offering greater potential to overcome the intrinsic limitations of undoped g-C_3N_4 and develop more efficient photocatalysts.

3.4. Metal Doping

Incorporating metal elements into g-C_3N_4 has proven to be an effective strategy for enhancing its photocatalytic properties. By modifying the material's band structure and surface characteristics, metal doping significantly improves visible light absorption, suppresses electron–hole recombination, and boosts overall catalytic activity [50]. The method of doping and the specific chemical state of the metal ion play crucial roles in determining the performance enhancements. Yang et al. [51] synthesized ultrathin cobalt-doped g-C_3N_4 nanosheets through a simple in situ thermal polymerization of melamine and cobalt nitrate. Various characterization techniques, including XRD, FTIR, and TEM, confirmed the successful integration of Co atoms. Electrochemical studies showed enhanced photocurrent response and reduced charge transfer resistance. The optimal sample, with 1 wt.% cobalt, achieved a hydrogen production rate 3.2 times greater than that of undoped bulk g-C_3N_4. This was primarily due to shorter charge transport paths in the nanosheets and the formation of Co–N coordination sites, which facilitated charge separation and transfer. Structurally, g-C_3N_4 is composed of a heptazine-based framework with nitrogen-rich cavities, making it highly receptive to metal ion coordination. When metal atoms are introduced,

they can bind within these cavities, forming stable metal–nitrogen bonds. This not only modifies the electronic structure by narrowing the bandgap but also improves the material's optical absorption and charge transport properties. A diverse range of metal dopants including Na, K, Fe, Co, Cu [52–57] etc. have been explored to tailor g-C_3N_4 photocatalytic behavior. For example, Mn-doped g-C_3N_4 demonstrated enhanced electronic conductivity and adjustable redox properties due to Mn–N–C bonding. These structural changes enabled full water splitting with a hydrogen evolution rate of 695.1 $\mu mol \cdot g^{-1} \cdot h^{-1}$, along with excellent operational stability.

In another study, Li et al. [58] introduced indium into the g-C_3N_4 lattice. The In atoms occupied the cavity sites of the structure, leading to an increase in surface area and more efficient charge carrier separation. As a result, the photocatalytic hydrogen production rate increased by nearly threefold compared to the undoped material. Overall, metal doping presents a powerful tool for fine-tuning the structural and electronic properties of g-C_3N_4. Through appropriate selection and integration of metal ions, the photocatalytic efficiency of g-C_3N_4 can be significantly improved, making it a more viable candidate for sustainable hydrogen production and other solar-driven applications.

3.5. Cocatalyst Modification

While graphitic carbon nitride (g-C_3N_4) has emerged as a promising photocatalyst, its performance in hydrogen production remains limited due to rapid recombination of photogenerated charge carriers. To overcome this challenge, researchers have increasingly turned to cocatalyst integration as an effective strategy. These cocatalysts not only promote the separation and migration of charge carriers but also provide active surface sites that facilitate the hydrogen evolution reaction (HER). Noble metals like platinum (Pt), palladium (Pd), silver (Ag), and gold (Au) have long been recognized as highly efficient cocatalysts. They play a crucial role in boosting the photocatalytic activity of g-C_3N_4 by enhancing electron transfer and suppressing recombination. Beyond these elemental metals, compound-based cocatalysts such as PtS_2 and Rh_xP have also shown promising results in recent studies. For example, Hu et al. [59] developed a g-C_3N_4 photocatalyst modified with atomically dispersed platinum. The Pt atoms formed Pt–N bonds with g-C_3N_4, acting as effective electron conduits. This configuration significantly shortened the distance for electron transport, leading to a notable increase in hydrogen evolution activity—up to 573.6 $\mu mol \cdot g^{-1} \cdot h^{-1}$ nearly 94 times that of pristine g-C_3N_4. In another study, Tian et al. [60] utilized gold nanorods (Au NRs) to create a plasmonic g-C_3N_4 hybrid. These nanorods are capable of generating energetic "hot" electrons when exposed to visible or near-infrared (NIR) light. The system achieved a hydrogen evolution rate of 350.6 $\mu mol \cdot g^{-1} \cdot h^{-1}$ under visible light, significantly outperforming Pt/g-C_3N_4, and also displayed measurable NIR activity, thanks to enhanced light absorption from the nanorods' surface plasmon resonance effects. Similarly, Chen et al. [61] prepared a silver quantum dot-decorated g-C_3N_4 photocatalyst using a straightforward one-step method. The ultra-small Ag dots (~0.5 nm) were evenly distributed across the surface, effectively extending light absorption into the visible range and serving as efficient electron sinks. This modification led to a 4.6-fold increase in hydrogen generation compared to the unmodified g-C_3N_4. Despite their excellent performance, noble metal cocatalysts come with drawbacks namely, high cost and limited availability which restrict their use in large-scale or commercial applications. As a result, research has increasingly focused on earth-abundant and cost-effective alternatives. These include:

- Base metals such as nickel (Ni), copper (Cu), cobalt (Co), and iron (Fe) [62]
- Metal hydroxides like $Ni(OH)_2$, $Cu(OH)_2$, $Co(OH)_2$, and $Fe(OH)_3$
- Metal oxides including Cu_2O, NiO, CoO, and Co_3O_4
- Transition metal phosphides such as CoP, Co_2P, Ni_2P, FeP, and Cu_2P [62]

Mahzoon et al. [63] reported a notable example using $Cu(OH)_2$ as a cocatalyst. The resulting 4$Cu(OH)_2$/g-C_3N_4 composite achieved a hydrogen production rate of 187 $\mu mol \cdot g^{-1} \cdot h^{-1}$, 31 times higher than that of g-C_3N_4 alone. Their synthesis method, assisted by ultrasonication, improved the number of active surface sites and enhanced charge transfer between g-C_3N_4 and the cocatalyst. This conclusion was well-supported by photoluminescence, photocurrent, and impedance spectroscopy analyses. In summary, modifying g-C_3N_4 with cocatalysts whether noble metals or earth-abundant materials plays a critical role in unlocking its full photocatalytic potential. While noble metals remain the benchmark for performance, the search for scalable, low-cost alternatives is rapidly gaining ground and yielding promising results for sustainable hydrogen production.

3.6. Heterojunction Construction

A major bottleneck in improving the efficiency of photocatalysts lies in the rapid recombination of photogenerated electrons and holes. This process significantly limits the material's ability to drive useful chemical reactions. To tackle this issue, researchers have focused on building heterojunction structures combinations of two different semiconductors which can greatly enhance charge separation and transfer, resulting in better photocatalytic performance.

The photocatalytic performance of pristine g-C_3N_4 is limited due to its high charge carrier recombination rate and narrow visible light absorption range. To address these challenges, g-C_3N_4-based heterojunctions have been developed, which enhance charge separation and broaden light absorption, resulting in improved photocatalytic activity.

A wide range of materials have been integrated with g-C_3N_4 to form heterojunctions, including carbon-based materials (e.g., graphene, carbon nanotubes, fullerenes), metal oxides (TiO_2, SnO_2, ZnO, $NiFe_2O_4$, Fe_2O_3), metal sulfides (CdS, ZnS, MoS_2), bismuth compounds ($BiPO_4$, $BiVO_4$, Bi_2WO_6), silver-based materials (Ag_2O, Ag_3PO_4, Ag_3VO_4), and complex oxides (Zn_2GeO_4, $SrTiO_3$). these combinations are designed to promote charge transfer and reduce recombination by aligning their energy bands appropriately with g-C_3N_4 [36,64].

Heterojunctions are classified based on the relative positions of the conduction and valence bands:

- Type I (Figure 4A): The conduction band of one semiconductor lies above, and its valence band below, those of the other. Under light irradiation, electrons and holes tend to accumulate in the narrower band gap material, but this structure often shows poor charge separation, limiting redox efficiency [65].
- Type II (Figure 4B): Both the conduction and valence bands of one semiconductor are lower than those of the other, enabling directional transfer of electrons and holes to opposite sides. This efficient charge separation enhances photocatalytic activity. For example, Roy et al. (2021) developed a TiO_2/ultrathin g-C_3N_4 heterostructure via in situ thermal exfoliation, achieving a redshift (~0.13 eV) in the absorption edge and improved light harvesting. Chen et al. synthesized a 3D hollow tubular g-C_3N_4/$ZnIn_2S$ g-C_3N_4 heterojunction, which exhibited a high H_2 production rate of 20,738 $\mu mol \cdot g^{-1} \cdot h^{-1}$ [66]. Fan et al. developed a NiS-Mn_2SnS_4/g-C_3N_4 composite via a simple physical mixing method and calcination process and found that under 300 W xenon lamp illumination, the NiS-Mn_2SnS_4/g-C_3N_4 composite shows a hydrogen evolution rate of 7672.45 $\mu mol \cdot g^{-1} \cdot h^{-1}$, which is 3.76, 59.74, and 254.64 times higher than the bare g-C_3N_4, NiS, and Mn_2SnS_4, respectively [67].
- Type III (Figure 4C): The conduction and valence bands of the two semiconductors do not overlap, preventing charge transfer across the interface and offering minimal improvement in photocatalytic performance [63].
- Z-scheme heterojunction (Figure 4D): A properly designed semiconductor heterojunction can improve light absorption and accelerate electron–hole separation, as seen in Type-II structures, but its photocatalytic oxidation ability remains limited. To overcome this, Z-scheme heterojunctions have been developed [68], classified into binary and ternary types [69]. In the binary Z-scheme (Figure 4D), semiconductor 2 has more positive CB and VB potentials than semiconductor 1, enhancing both reduction and oxidation capabilities. For instance, Zhao et al. synthesized CeO_2/g-C_3N_4 heterojunctions via one-step in situ pyrolysis, yielding 3D CeO_2 mesoporous nanospheres with 2D g-C_3N_4 sheets. The optimized CeO_2/g-C_3N_4-6 exhibited a hydrogen evolution rate of 1240.9 $\mu mol \cdot g^{-1} \cdot h^{-1}$ about 5.2 times higher than pure CeO_2 [70]. He et al., synthesized cobalt oxide/tubular-like carbon nitride (CoOx/TCN) Z-scheme by a high-temperature calcination method and studied the photocatalytic hydrogen production. Construction of CoOx/tubular g-C_3N_4 Z-scheme heterojunction for synergistically enhanced photocatalytic hydrogen production [71].
- S-scheme heterojunction: g-C_3N_4 homojunctions are known for efficient photocatalysis, but conventional Type-II and Z-scheme structures suffer from weakened redox potentials and require improved electron transport. Inspired by the S-scheme concept [72]. Li et al. fabricated P-doped ultrathin g-C_3N_4/In_2S_3 S-scheme heterojunction by urea recrystallization and found that the maximum a hydrogen production rate of 12,387 $\mu mol \cdot g^{-1} \cdot h^{-1}$ [73]. Wang et al., designed Co_9S_8/Flower-like g-C_3N_4 van der Waals Heterojunction (S-Scheme) by in-situ growth method and notably, achieved the highest H_2 evolution of 948.04 $\mu mol \cdot g^{-1} \cdot h^{-1}$ [74]. Table 1 present hydrogen production using different g-C_3N_4 based photocatalysts

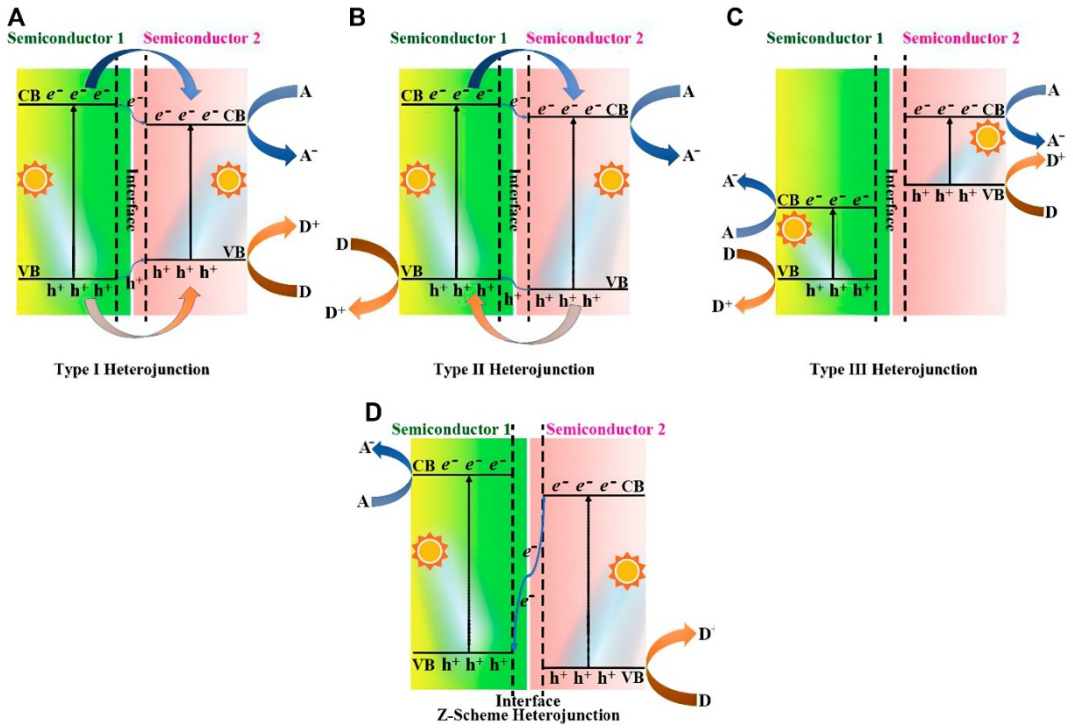

Figure 4. Schematic representation of different types of hetero-junction photocatalysts: (**A**) Type I, (**B**) Type II, (**C**) Type III, (**D**) Z-scheme hetrojunction. Reproduced with permission from [36]. © 2022 by the authors, licensed under CC BY 4.0.

Table 1. Different g-C_3N_4 based photocatalysts for hydrogen production.

Photocatalysts	Fabrication Process	Precursors of g-C_3N_4	Photocatalytic Performance (μmol·g^{-1}·h^{-1})	References
CdS/RGO/g-C_3N_4	Hydrothermal	Melamine	1980.2	[75]
g-C_3N_4/Pt	Impregnation	Melamine	2932.8	[76]
K-doped g-C_3N_4	Hydrothermal	Melamine	919.5	[77]
ZnS/g-C_3N_4 heterojunction	Situ Calcination	Melamine	713.68	[78]
N/g-C_3N_4	Calcination	Urea	64	[79]
g-C_3N_4/α-Fe_2O_3	One-pot hydrothermal	Melamine	77.6	[80]
g-C_3N_4/Ag_2S	Precipitation	Urea	10	[81]
g-C_3N_4/TiO_2	Vapor deposition	Melamine	513	[82]
g-C_3N_4/AuPd	Situ-chemical solution deposition	Melamine	107	[83]
g-C_3N_4/Nb_2O_5	Solvothermal	Urea	1710.04	[84]
g-C_3N_4/SnO_2	Chemical	Melamine	900	[85]
g-C_3N_4/ZnS	Precipitation	Urea	194	[86]
g-C_3N_4/NiS_2	Impregnation	Melamine	116.3435	[87]
g-C_3N_4/WO_3	Hydrothermal	Urea	48.2	[88]
g-C_3N_4/$CuFe_2O_4$	One-pot calcination	Urea	76	[89]

3.7. Photocatalytic Testing Standards

Accurate comparison of photocatalytic hydrogen evolution rates requires standardized testing protocols. Reported activities for g-C_3N_4 based systems often vary due to differences in light sources, sacrificial agents, and normalization criteria. Typically, a 300 W Xe lamp equipped with a UV cut-off filter ($\lambda > 420$ nm) is used as the visible-light source, and the light intensity should be calibrated using a photo-radiometer. Photocatalytic reactions are commonly conducted in aqueous solutions containing sacrificial electron donors such as triethanolamine (TEOA), methanol, or Na_2S/Na_2SO_3 under continuous stirring and constant temperature (≈25 °C) [75–85]. The evolved hydrogen is quantified by gas chromatography (GC) equipped with a thermal conductivity detector (TCD). For fair comparison, the hydrogen evolution rate should be normalized to the catalyst mass and expressed as μmol·g^{-1}·h^{-1}. Some studies also report apparent quantum efficiency (AQE) values to account for photon

utilization. Establishing and following such standardized testing conditions is essential to ensure reproducibility, minimize measurement discrepancies, and enable objective evaluation of photocatalytic performance across different g-C_3N_4 based systems.

4. Conclusions and Future Outlook

This review has provided a comprehensive overview of the synthesis strategies and photocatalytic performance of g-C_3N_4-based composite materials for hydrogen production, emphasizing their substantial potential as efficient photocatalysts for solar-driven water splitting. Despite their intrinsic advantages such as chemical stability, tunable band structure, and low intrinsic cost pristine g-C_3N_4 still suffers from limitations, including rapid charge carrier recombination, low specific surface area, and limited visible-light absorption. To overcome these challenges, numerous structural modification strategies have been explored, including morphology engineering, elemental doping, cocatalyst integration, and heterojunction construction. Advanced approaches such as single-atom catalysis, defect engineering, and plasmonic enhancement have further contributed to improving charge separation, surface reactivity, and light utilization efficiency.

Morphological tuning through nano-structuring and surface modification effectively increases the surface area and promotes charge transport. Elemental doping both metallic and non-metallic—facilitates band-gap tuning and enhances photon absorption and catalytic site availability. Heterojunction engineering, particularly the construction of type-II and Z-scheme architectures, has proven highly effective in accelerating interfacial charge transfer and suppressing recombination. In addition, defect modulation and plasmonic coupling provide new routes to extend light absorption into the visible–near-infrared region, offering further improvements in photocatalytic performance. Collectively, these advancements contribute to enhanced interfacial contact, increased catalytic activity, and superior overall hydrogen evolution efficiency.

Cost, Scalability, and Sustainability Considerations: While g-C_3N_4 is inherently low-cost and metal-free, the practical deployment of its modified composites depends strongly on synthesis scalability and environmental compatibility. Conventional synthesis routes such as high-temperature thermal polymerization, hydrothermal, and chemical vapor deposition methods are often energy-intensive, batch-limited, and dependent on toxic precursors or solvents, leading to high operational costs and environmental burden. In contrast, emerging green synthesis technologies, including microwave-assisted polymerization, mild solvothermal processing, and bio-templating, have demonstrated reduced energy consumption, shorter reaction times, and improved product uniformity. For industrial translation, continuous-flow or plasma-assisted synthesis systems could provide scalable, energy-efficient, and reproducible production pathways. Furthermore, minimizing the use of noble-metal cocatalysts and adopting earth-abundant, non-toxic alternatives are essential to reduce cost and align with sustainable development goals. Therefore, future research should focus on developing low-carbon, economically viable, and environmentally benign synthesis processes that retain high photocatalytic efficiency while ensuring large-scale manufacturability.

Future progress in g-C_3N_4-based photocatalysis can be accelerated through several key directions. (i) Machine learning–guided materials discovery can enable rapid identification of optimal dopants, heterojunction architectures, and synthesis parameters through data-driven correlations between structure and activity. (ii) In situ and operando characterization techniques are crucial for elucidating charge transfer dynamics, reaction intermediates, and degradation pathways under realistic conditions, providing deeper mechanistic insights. (iii) Coupled photocatalytic systems integrating hydrogen evolution with CO_2 reduction or environmental remediation offers dual functionality and improved solar-to-chemical conversion efficiency. Integrating these strategies within scalable and sustainable synthesis frameworks will be critical for bridging the gap between laboratory research and industrial implementation.

Overall, through rational structural design, environmentally conscious process development, and interdisciplinary integration, g-C_3N_4-based photocatalysts are expected to play a pivotal role in next-generation sustainable hydrogen production and broader solar-to-chemical energy conversion technologies.

Author Contributions

Y.M.H.: conceptualization, investigation, writing-original draft preparation, reviewing and editing, A.A.Y.: writing-original draft preparation, reviewing and editing, S.M.: reviewing and editing, A.H.I.M.: conceptualization, A.F.: conceptualization, supervision, methodology, C.T.: conceptualization, supervision, methodology. All authors have read and agreed to the published version of the manuscript.

Funding

This research received no external funding.

Institutional Review Board Statement

Not applicable.

Informed Consent Statement

Not applicable.

Data Availability Statement

Data are contained within the article.

Acknowledgments

The authors gratefully acknowledge the support provided by the United Arab Emirates University under the Research Grant Code: 12R304.

Conflicts of Interest

The authors declare no conflict of interest.

Use of AI and AI-Assisted Technologies

No AI tools were utilized for this paper.

References

1. Liao, G.; Li, C.; Liu, S.Y.; et al. Emerging frontiers of Z-scheme photocatalytic systems. *Trends Chem.* **2022**, *4*, 111–127.
2. Reddy, P.B.; Ravindran, E.; Rosaiah, P.; et al. Hierarchical copper indium sulfide and MXene composites: Synergistic effects for enhanced lithium-ion battery performance and photocatalytic hydrogen production. *Ceram. Int.* **2025**, *51*, 51723–51733.
3. Yadav, A.A.; Hunge, Y.M.; Dhodamani, A.G.; et al. Hydrothermally Synthesized Ag@MoS_2 Composite for Enhanced Photocatalytic Hydrogen Production. *Catalysts* **2023**, *13*, 716.
4. Hunge, Y.M.; Yadav, A.A.; Kang, S.W.; et al. Role of nanotechnology in photocatalysis application. *Recent Pat. Nanotechnol.* **2023**, *17*, 5–7.
5. Hunge, Y.M.; Yadav, A.A.; Kang, S.W.; et al. Visible light activated MoS_2/ZnO composites for photocatalytic degradation of ciprofloxacin antibiotic hydrogen production. *J. Photochem. Photobio. A Chem.* **2023**, *434*, 114250.
6. Hunge, Y.M.; Yadav, A.A.; Kang, S.W.; et al. Facile synthesis of multitasking composite of Silver nanoparticle with Zinc oxide for 4-nitrophenol reduction, photocatalytic hydrogen production, and 4-chlorophenol degradation. *J. Alloys Compd.* **2022**, *928*, 167133.
7. Yadav, A.A.; Hunge, Y.M.; Kang, S.W. Visible Light-Responsive CeO_2/MoS_2 Composite for Photocatalytic Hydrogen Production. *Catalysts* **2022**, *12*, 1185.
8. Yadav, A.A.; Hunge, Y.M.; Kang, S.W. Porous nanoplate-like tungsten trioxide/reduced graphene oxide catalyst for sonocatalytic degradation and photocatalytic hydrogen production. *Surf. Interf.* **2021**, *24*, 101075.
9. Yadav, A.A.; Hunge, Y.M.; Kang, S.W. Spongy ball-like copper oxide nanostructure modified by reduced graphene oxide for enhanced photocatalytic hydrogen production. *Mater. Res. Bull.* **2021**, *133*, 111026.
10. Kumar, Y.A.; Kalla RM, N.; Al-Sehemi, A.G.; et al. Emerging group-VA 2D materials: Antimonene bismuthene for nanoelectronics energy storage. *J. Alloys Compd.* **2025**, *1044*, 184331.
11. Hunge, Y.M.; Yadav, A.A.; Mathe, V.L. Photocatalytic hydrogen production using TiO_2 nanogranules prepared by hydrothermal route. *Chem. Phys. Lett.* **2019**, *731*, 136582.
12. Liao, G.; Li, C.; Li, X.; Fang, B. Emerging polymeric carbon nitride Z-scheme systems for photocatalysis. *Cell Rep. Phys. Sci.* **2021**, *2*, 100355.
13. Jia, X.; Song, Z.Q.; Zhang, J.Q.; et al. A ternary Z-scheme heterojunction composite CdS@Ce-MOF/g-C_3N_4 for efficient photocatalytic hydrogen evolution. *Int. J. Hydrogen Energy* **2025**, *139*, 25–35.
14. Majumder, S.; Yadav, A.A.; Gomez, L.A.M.; et al. Unlocking clean energy: Exploring $FeVO_4$ nanopebble thin film as an outstanding photoanode for efficient water splitting. *J. Alloys. Compd.* **2024**, *1002*, 175391.
15. Kudo, A.; Miseki, Y. Heterogeneous photocatalyst materials for water splitting. *Chem. Soc. Rev.* **2009**, *38*, 253–278.

16. Majumder, S.; Yadav, A.A.; Palanisamy, A.K.; et al. Design and optimization of $FeVO_4/Fe_2TiO_5$ heterojunction photoanode for efficient photoelectrochemical water splitting. *Ceram. Int.* **2025**, *51*, 2536–2546.
17. Xiao, M.; Luo, B.; Wang, S.C.; et al. Solar energy conversion on g-C_3N_4 photocatalyst: Light harvesting charge separation surface kinetics. *J. Energy Chem.* **2018**, *27*, 1111–1123.
18. Tan, M.; Yu, C.; Li, J.; et al. Engineering of g-C_3N_4-based photocatalysts to enhance hydrogen evolution. *Adv. Colloid Interface Sci.* **2021**, *295*, 1024, 88.
19. Chen, H.; Fan, Z.; Zhang, Z.-C.; et al. Synthesis and modification of g-C_3N_4 semiconductor catalysts for photocatalytic hydrogen evolution: A review. *Prog. Nat. Sci. Mater. Int.* **2025**, *35*, 449–468.
20. Wang, X.; Maeda, K.; Thomas, A.; et al. A metal-free polymeric photocatalyst for hydrogen production from water under visible light. *Nat. Mater.* **2008**, *8*, 76–80.
21. Gomari, A.K.; Hafeez, Y.H.; Mohammed, J.; et al. A recent development future prospect of g-C_3N_4-based photocatalyst for stable hydrogen (H_2) generation via photocatalytic water-splitting. *Int. J. Hydrogen Energy* **2024**, *85*, 598–624.
22. Zhang, Y.; Wen, D.; Sun, W.; et al. State-of-the-art evolution of g-C_3N_4-based photocatalytic applications: A critical review. *Chin. J. Struct. Chem.* **2024**, *43*, 100469.
23. Lin, T.H.; Chang, Y.H.; Chiang, K.P.; et al. Nanoscale multidimensional $Pd/TiO_2/g\text{-}C_3N_4$ catalyst for efficient solar-driven photocatalytic hydrogen production. *Catalysts* **2021**, *1*, 59.
24. Ma, S.H.; Wang, W.X. Preparation and photocatalytic hydrogen evolution of g-C_3N_4/ZnO composite. *E3S Web. Conf.* **2020**, *165*, 05007.
25. Zahra, M.; Farshad, Y.; Kourosh, H.T.; et al. Photocatalytic hydrogen evolution under visible light using $MoS_2/g\text{-}C_3N_4$ nano-photocatalysts. *Catal. Lett.* **2023**, *154*, 1255–1269.
26. Chen, Q.; Huang, J.; Chu, D.; et al. Inhibiting photogenerated electron-hole recombination in double metal phosphides decorated g-C_3N_4 nanosheets by work function gradient for improved hydrogen production. *Int. J. Hydrogen Energy* **2024**, *90*, 1023–1030.
27. Bao, T.; Li, X.; Li, S.; et al. Recent advances of graphitic carbon nitride (g-C_3N_4) based materials for photocatalytic applications: A review. *Nano. Mater. Sci.* **2025**, *7*, 145–168.
28. Bhanderi, D.; Lakhani, P.; Modi, C.K. Graphitic carbon nitride (g-C_3N_4) as an emerging photocatalyst for sustainable environmental applications: A comprehensive review. *RSC Sustain.* **2024**, *2*, 265–287.
29. Ma, D.D.; Zhang, Z.M.; Zhou, Y.J.; et al. The progress of g-C_3N_4 in photocatalytic H_2 evolution: From fabrication to modification. *Coord. Chem. Rev.* **2024**, *500*, 215489.
30. Kamble, B.B.; Sharma, K.K.; Sonawane, K.D.; et al. Graphitic carbon nitride-based electrochemical sensors: A comprehensive review of their synthesis, characterization, and applications. *Adv. Colloid. Interface. Sci.* **2024**, *333*, 103284.
31. Xie, Z.B.; Wang, C.; Wu, F.Q.; et al. Loading silver nanoclusters onto g-C_3N_4 by formamide-assisted in-situ strategy to achieve efficient photocatalytic water splitting for hydrogen production. *J Photochem. Photobiol. Chem.* **2025**, *462*, 116275.
32. Dankawu, U.; Hafeez, Y.H.; Ndikilar, E.C.; et al. Recent advances perspective of g-C_3N_4-based materials for efficient solar fuel (hydrogen) generation via photocatalytic water-splitting. *Int. J. Hydrogen Energy* **2024**, *67*, 1218–1242.
33. Mamba, G.; Mishra, A. Graphitic carbon nitride (g-C_3N_4) nanocomposites: A new and exciting generation of visible light driven photocatalysts for environmental pollution remediation. *Appl. Catal. B Environ.* **2016**, *198*, 347–377.
34. Kornel, K.; Marta, K.; Artur, K. Two-stage closed sinus lift: A new surgical technique for maxillary sinus floor augmentation. *Cell Tissue Bank* **2015**, *16*, 579–585.
35. Khac, B.T.; Nguyen, T.L.; Pham, V.V. Review of g-C_3N_4-based photocatalysts for Amoxicillin photocatalytic degradation. *J. Water Proc. Eng.* **2024**, *67*, 106257.
36. Gao, R.-H.; Ge, Q.; Jiang, N.; et al. Graphitic carbon nitride (g-C_3N_4)-based photocatalytic materials for hydrogen evolution. *Front. Chem.* **2022**, *10*, 1048504. https://doi.org/10.3389/fchem.2022.1048504.
37. Wang, W.; Yu, J.C.; Shen, Z.; et al. g-C_3N_4 quantum dots: Direct synthesis, upconversion properties and photocatalytic application. *Chem. Commun.* **2014**, *50*, 10148–10150.
38. Bashir, H.; Yi, X.Y.; Yuan, J.L.; et al. Highly ordered TiO_2 nanotube arrays embedded with g-C_3N_4 nanorods for enhanced photocatalytic activity. *J. Photochem. Photobiol. A Chem.* **2019**, *382*, 111930.
39. Shi, Y.X.; Li, L.L.; Sun, H.R.; et al. Engineering ultrathin oxygen-doped g-C_3N_4 nanosheet for boosted photoredox catalytic activity based on a facile thermal gas-shocking exfoliation effect. *Sep. Purif. Technol.* **2022**, *292*, 121038.
40. Chen, X.; Shi, R.; Chen, Q.; et al. Three-dimensional porous g-C_3N_4 for highly efficient photocatalytic overall water splitting. *Nano Energy* **2019**, *59*, 644–650.
41. Khan, A.M.; Mutahir, S.; Shaheen, I.; et al. Recent advances over the doped g-C_3N_4 in photocatalysis: A review. *Coord. Chem. Rev.* **2025**, *522*, 216227.

42. Yang, S.; Vanish, K.; Ki-Hyun, K. The assessment of graphitic carbon nitride (g-C_3N_4) materials for hydrogen evolution reaction: Effect of metallic and non-metallic modifications. *Separ. Purif. Technol.* **2023**, *305*, 122413.
43. Nagar, P.O.; Chouhan, N. Non-metal doped graphitic carbon nitride (g-C_3N_4): Prospects review on hydrogen generation via water splitting. *Int. J. Hydrogen Energy* **2024**, *96*, 533–565.
44. Yue, D.; Raj, M.N.S.; Kumar, V.J.; et al. History of metal free g-C_3N_4 photocatalysts for hydrogen production. *Diam. Relat. Mater.* **2024**, *146*, 111228.
45. Zhan, W.; Yang, N.; Zhou, T.; et al. Boron doping induced photocatalytic active site shift in ultrathin porous g-C_3N_4 for significant boosting H_2 production. *Int. J. Hydrogen Energy* **2024**, *92*, 907–916.
46. Cao, J.; Jing, X.L.; Ma, Z.Y.; et al. One-step synthesis of C quantum dots/C doped g-C_3N_4 photocatalysts for visible-light-driven H2 production from water splitting. *J. Phys. Appl. Phys.* **2022**, *55*, 444008.
47. Wang, W.K.; Wei, S.; Hu, Y.; et al. Fast carrier separation induced by the metal-like O-doped MoS_2/CoS cocatalyst for achieving photocatalytic and photothermal hydrogen production. *Chem. Eng. J.* **2024**, *493*, 152516.
48. Khursheed, A.; Mohd, Q.K.; Ali, A.; et al. Sulfur-doped graphitic-carbon nitride (S@g-C_3N_4) as bi-functional catalysts for hydrazine sensing and hydrogen production applications. *Synth. Met.* **2022**, *288*, 117100.
49. Hussain, A.S.; Hu, J.; Liu, H.; et al Preparation of C-doped g-C_3N_4 by Co-polycondensation of melamine sucrose for improved photocatalytic H_2 evolution. *Int. J. Hydrogen Energy* **2024**, *87*, 705–712.
50. Leila, H.; Clement, M.; Valerie, C.; et al. Influence of low level of non-metal doping on g-C_3N_4 performance for H_2 production from water under solar light irradiation. *Int. J. Hydrogen Energy* **2024**, *51*, 285–300.
51. Yang, X.; Tian, Z.; Chen, Y.F.; et al. In situ synthesis of 2D ultrathin cobalt doped g-C_3N_4 nanosheets enhances photocatalytic performance by accelerating charge transfer. *J. Alloys. Compd.* **2021**, *859*, 157754.
52. Zhang, L.S.; Ding, N.; Hashimoto, M.; et al. Sodium-doped carbon nitride nanotubes for efficient visible light-driven hydrogen production. *Nano. Res.* **2018**, *11*, 2295–2309.
53. Gao, L.F.; Wen, T.; Xu, J.Y.; et al. Iron-doped carbon nitride-type polymers as homogeneous organocatalysts for visible light-driven hydrogen evolution. *Acs. Appl. Mater. Inter.* **2016**, *8*, 617–624.
54. Song, X.F.; Tao, H.; Chen, L.X.; et al. Synthesis of Fe/g-C_3N_4 composites with improved visible light photocatalytic activity. *Mater. Lett.* **2014**, *116*, 265–267.
55. Wan, Y.; Wang, H.; Liu, J.; et al. Removal of polyethylene terephthalate plastics waste via Co–CeO_2 photocatalyst–activated peroxymonosulfate strategy. *Chem. Eng. J.* **2024**, *479*, 147781.
56. Xiong, T.; Cen, W.L.; Zhang, Y.X.; et al. Bridging the g-C_3N_4 Interlayers for enhanced photocatalysis. *ACS Catal.* **2016**, *6*, 2462–2472.
57. Zhou, Y.Y.; Zhang, L.; Wang, W.Z. Direct functionalization of methane into ethanol over copper modified polymeric carbon nitride via photocatalysis. *Nat. Commun.* **2019**, *10*, 506.
58. Li, H.P.; Xia, Y.G.; Liang, Z.W.; et al. Energy band engineering of polymeric carbon nitride with indium doping for high enhancement in charge separation and photocatalytic performance. *ACS Appl. Energy Mater.* **2020**, *3*, 377–386.
59. Hu, Y.D.; Qu, Y.T.; Zhou, Y.S.; et al. Single Pt atom-anchored C_3N_4: A bridging Pt-N bond boosted electron transfer for highly efficient photocatalytic H_2 generation. *Chem. Eng. J.* **2021**, *412*, 128749.
60. Tian, H.Y.; Liu, X.; Liang, Z.Q.; et al. Gold nanorods/g-C_3N_4 heterostructures for plasmon-enhanced photocatalytic H_2 evolution in visible near-infrared light. *J. Colloid Interface Sci.* **2019**, *557*, 700–708.
61. Chen, T.; Quan, W.; Yu, L.; et al. One step synthesis visible-light-driven H_2 production from water splitting of Ag quantum dots/g-C_3N_4 photocatalysts. *J. Alloys Compd.* **2016**, *686*, 628–634.
62. Ren, W.; Wang, J.; Zheng, X.; et al. Transition metal phosphides (Fe2P, Co2P, and Ni_2P) modified CdS nanorods for efficient photocatalytic H_2 Evolution. *ACS Appl. Nano Mater.* **2024**, *7*, 22137–22146
63. Mahzoon, S.; Haghighi, M.; Nowee, S.M. Sonoprecipitation fabrication of enhanced electron transfer $Cu(OH)_2$/g-C_3N_4 nanophotocatalyst with promoted H_2 Production activity under visible light irradiation. *Renew. Energy* **2020**, *150*, 91–100.
64. Reza, G.M.; Dinh, C.T.; Beland, F.; et al. Nanocomposite heterojunctions as sunlight-driven photocatalysts for hydrogen production from water splitting. *Nanoscale* **2015**, *7*, 8187–8208.
65. Fu, J.; Yu, J.; Jiang, C.; Cheng, B. g-C_3N_4-based heterostructured photocatalysts. *Adv. Energy Mat.* **2018**, *8*, 1701503–1701531.
66. Chen, Z.H.; Guo, F.; Sun, H.; et al. Well-designed three-dimensional hierarchical hollow tubular g-C_3N_4/$ZnIn_2S_4$ nanosheets heterostructure for achieving efficient visible-light photocatalytic hydrogen evolution. *J. Colloid Interface Sci.* **2022**, *607*, 1391–1401.
67. Fan, J.; Yang, Y.; Liu, J.; et al. Constructed NiS-Mn_2SnS_4/g-C_3N_4 dual-stage type-II heterojunction with high-specific-surface-area for synergistically enhanced photocatalytic hydrogen production performance. *Fuel* **2026**, *405*, 136702.
68. Xu, Z.; Shi, Y.X.; Li, L.L.; et al. Fabrication of 2D/2DZ-scheme highly crystalline carbon nitride/δ-Bi_2O_3 heterojunction photocatalyst with enhanced photocatalytic degradation of tetracycline. *J. Alloys Compd.* **2022**, *895*, 16266.
69. Maeda, K. Z-scheme water splitting using two different semiconductor photocatalysts. *ACS Catal.* **2013**, *3*, 1486–1503.

70. Zhao, S.; Xu, J.; Mao, M.; et al. Protonated g-C_3N_4 cooperated with Co-MOF doped with Sm to construct 2D/2D heterojunction for integrated dye-sensitized photocatalytic H_2 evolution. *J. Colloid Interface Sci.* **2021**, *583*, 435–447.
71. He, J.; Zou, X.; Dong, Y.; et al. Construction of CoOx/tubular C_3N_4 Z-scheme heterojunction for synergistically enhanced photocatalytic hydrogen production. *Renew. Ener*gy **2026**, *256*, 124274.
72. Xu, Q.; Zhang, L.; Cheng, B.; et al. S-scheme heterojunction photocatalyst. *Chem* **2020**, *6*, 1543–1559.
73. Li, Y.; Yang, H.; Li, W.; et al. P-doped ultrathin g-C_3N_4/In_2S_3 S-scheme heterojunction enhances photocatalytic hydrogen production and degradation of ofloxacin. *Phys. B* **2024**, *685*, 416053.
74. Wang, Y.; Lin, H.; Zong, J.; et al. Interface Design of S Scheme Co_9S_8/Flower-like g-C_3N_4 van der Waals Heterojunction with Enhanced Photocatalytic Hydrogen Production and Tetracycline Hydrochloride Degradation. *Chin. J. Struct. Chem.* **2025**, 100798. https://doi.org/10.1016/j.cjsc.2025.100798.
75. Jo, W.-K.; Selvam, N.C.S. Z-scheme CdS/g-C_3N_4 composites with RGO as an electron mediator for efficient photocatalytic H2 production and pollutant degradation. *Chem. Eng. J.* **2017**, *317*, 913–924.
76. Ou, M.; Wan, S.; Zhong, Q.; et al. Single Pt atoms deposition on g-C_3N_4 nanosheets for photocatalytic H_2 evolution or NO oxidation under visible light. *Int. J. Hydrogen Energy* **2017**, *42*, 27043–27054.
77. Sun, S.; Li, J.; Cui, J.; et al. Simultaneously engineering Kdoping exfoliation into graphitic carbon nitride (g-C_3N_4) for enhanced photocatalytic hydrogen production. *Int. J. Hydrogen Energy* **2019**, *44*, 778–787.
78. Hao, X.; Zhou, J.; Cui, Z.; et al. Zn-vacancy mediated electron-hole separation in ZnS/g-C_3N_4 heterojunction for efficient visible-light photocatalytic hydrogen production. *Appl. Catal. B. Environ.* **2018**, *229*, 41–51.
79. Zhou, Y.; Zhang, L.; Huang, W.; et al. N-doped graphitic carbon-incorporated g-C_3N_4 for remarkably enhanced photocatalytic H2 evolution under visible light. *Carbon* **2016**, *99*, 111–117.
80. Li, Y.-P.; Li, F.-T.; Wang, X.-J.; et al. Z-scheme electronic transfer of quantum-sized α-Fe_2O_3 modified g-C_3N_4 hybrids for enhanced photocatalytic hydrogen production. *Int. J. Hydrogen Energy* **2017**, *42*, 28327–28336.
81. Jiang, D.; Chen, L.; Xie, J.; et al. Ag_2S/g-C_3N_4 composite photocatalysts for efficient Pt-free hydrogen production. The co-catalyst function of Ag/Ag2S formed by simultaneous photodeposition. *Dalton Trans.* **2014**, *43*, 4878–4885.
82. Tan, Y.; Shu, Z.; Zhou, J.; et al. One-step synthesis of nanostructured g-C_3N_4/TiO_2 composite for highly enhanced visible-light photocatalytic H_2 evolution. *Appl. Catal. B. Environ.* **2018**, *230*, 260–268.
83. Han, C.; Gao, Y.; Liu, S.; et al. Facile synthesis of AuPd/g-C_3N_4 nanocomposite: An effective strategy to enhance photocatalytic hydrogen evolution activity. *Int. J. Hydrogen Energy* **2017**, *42*, 22765–22775.
84. Huang, Q.-Z.; Wang, J.-C.; Wang, P.-P.; et al. In-situ growth of mesoporous Nb_2O_5 microspheres on g-C_3N_4 nanosheets for enhanced photocatalytic H_2 evolution under visible light irradiation. *Int. J. Hydrogen Energy* **2017**, *42*, 6683–6694.
85. Zang, Y.; Li, L.; Li, X.; et al. Synergistic collaboration of g-C_3N_4/SnO_2 composites for enhanced visible-light photocatalytic activity. *Chem. Eng. J.* **2014**, *246*, 277–286.
86. Shi, F.; Chen, L.; Xing, C.; et al. ZnS microsphere/g-C_3N_4 nanocomposite photo-catalyst with greatly enhanced visible light performance for hydrogen evolution: Synthesis and synergistic mechanism study. *RSC Adv.* **2014**, *4*, 62223–62229.
87. Chen, F.; Yang, H.; Wang, X.; et al. Facile synthesis enhanced photocatalytic H_2-evolution performance of NiS_2-modified g-C_3N_4 photocatalysts Chin. *J. Catal.* **2017**, *38*, 296–304.
88. Hong, J.; Wang, Y.; Wang, Y.; et al. Noble-metal-free NiS/C_3N_4 for efficient photocatalytic hydrogen evolution from water. *ChemSusChem* **2013**, *6*, 2263–2268.
89. Cheng, R.; Fan, X.; Wang, M.; et al. Facile construction of $CuFe_2O_4$/g-C_3N_4 photocatalyst for enhanced visible-light hydrogen evolution. *RSC Adv.* **2016**, *6*, 18990–18995.